



RESEARCH ARTICLE

# Antibiofilm and anti-quorum properties of ethanolic leaf extracts of *Syzygium jambos* and *Psidium guajava* and their gel formulation for wound healing applications

Sandhya Kalathilparambil Santhosh<sup>1</sup> & Suma Sarojini<sup>2\*</sup>

Department of Life Sciences, CHRIST (Deemed to be University), Bengaluru 560 029, Karnataka, India

\*Email: [suma@christuniversity.in](mailto:suma@christuniversity.in)



## ARTICLE HISTORY

Received: 27 November 2024

Accepted: 24 December 2024

Available online

Version 1.0 : 09 March 2025

Version 2.0 : 01 April 2025



## Additional information

**Peer review:** Publisher thanks Sectional Editor and the other anonymous reviewers for their contribution to the peer review of this work.

**Reprints & permissions information** is available at [https://horizonepublishing.com/journals/index.php/PST/open\\_access\\_policy](https://horizonepublishing.com/journals/index.php/PST/open_access_policy)

**Publisher's Note:** Horizon e-Publishing Group remains neutral with regard to jurisdictional claims in published maps and institutional affiliations.

**Indexing:** Plant Science Today, published by Horizon e-Publishing Group, is covered by Scopus, Web of Science, BIOSIS Previews, Clarivate Analytics, NAAS, UGC Care, etc See [https://horizonepublishing.com/journals/index.php/PST/indexing\\_abstracting](https://horizonepublishing.com/journals/index.php/PST/indexing_abstracting)

**Copyright:** © The Author(s). This is an open-access article distributed under the terms of the Creative Commons Attribution License, which permits unrestricted use, distribution and reproduction in any medium, provided the original author and source are credited (<https://creativecommons.org/licenses/by/4.0/>)

## CITE THIS ARTICLE

Santhosh S K, Sarojini S. Antibiofilm and anti-quorum properties of ethanolic leaf extracts of *Syzygium jambos* and *Psidium guajava* and their gel formulation for wound healing applications. Plant Science Today. 2025; 12 (2): 1-13. <https://doi.org/10.14719/pst.6365>

## Abstract

Most bacterial species today have evolved with time and gained resistance to a wide range of antibiotics, primarily due to formation of biofilms and  $\beta$ -lactamases. Many phytochemicals have been explored for their ability to inhibit bacterial biofilms. The present study sheds light on antibiofilm properties of two such plants viz. *Psidium guajava* and *Syzygium jambos*, of the Myrtaceae family. They were found to be effective against four different biofilm forming pathogens - *Chromobacterium violaceum*, *Klebsiella pneumoniae*, *Pseudomonas aeruginosa* and *Staphylococcus aureus*. Synergistic use of the plant extracts showed slightly better antibacterial activity than a single extract. Quorum sensing being one of the key factors required for biofilm formation, the isolate *Chromobacterium violaceum* was used as the indicator organism to study the anti-quorum properties of the plant extracts. At 10 mg/mL, ethanolic extract of *S. jambos* inhibited violacein pigment the most (78.84%) and therefore can be considered as a quorum sensing inhibitor (QSI). Since silver nanoparticles (AgNPs) have become increasingly significant in the field of drug delivery, they may be utilized to coat implants to avoid subsequent infections in patients who have had implant surgery and to reduce biofilm development in pathogens. In the present study, five gels were formulated using plant extracts and AgNPs, of which two showed promising results in wound healing assay. The non-toxic nature of the synthesized gels has been verified by studies on L-929 mouse fibroblast cell lines, which opens the door for their prospective application as topical treatments to accelerate the healing process in both acute and chronic wounds. Given that *S. aureus* and *P. aeruginosa* are the most commonly isolated bacteria from diabetic foot ulcers, the resulting gels can considerably curb the spread of infection and gangrene and thus prevent amputation.

## Keywords

antibiofilm; anti-quorum; AgNPs; *Psidium guajava*; *Syzygium jambos*; wound healing

## Introduction

A self-produced extracellular polymeric substance encasing a well-organized group of bacteria that is highly resistant to traditional antimicrobial treatments is called a biofilm (1). This matrix facilitates bacterial adhesion to surfaces, posing significant threats to health and safety. Antibiotic resistance is conferred by the matrix through a variety of mechanisms, including the expression of resistant genes, limitation to antibiotic entry into

cells, growth rate reduction, and even host immunity counteraction. Penicillin was once considered a wonder drug or the miracle drug as it saved so many lives from bacterial infections that were fatal before its discovery. But eventually with the evolution of bacteria that can produce metallo beta lactamases (MBLs) and extended spectrum beta lactamases (ESBLs), these drugs started losing their efficacy in treating serious infections like septicemia, urinary tract infections (UTIs) and pneumonia caused by bacteria such as *K. pneumoniae*, *Pseudomonas aeruginosa*, *Escherichia coli* etc. The ability of some of these bacterial cells to form biofilms acts synergistically to confer antibiotic resistance along with the production of  $\beta$ -lactamases (2). The underlying principle behind biofilm formation is, however, quorum sensing. QS cell density-dependent control of gene expression is a crucial aspect of biofilm physiological development since biofilms typically include large concentrations of cells. It describes how quorum sensing molecules or small signalling molecules called autoinducers (AIs) diffuse between cells to sense population density (3). When the concentration of cells in a community is low, the concentration of AIs is low. Thus, it can be concluded that the concentration of cells and AIs are directly proportional. As the cell density increases, the concentration of AIs in the external environment increases and they diffuse back into the cell to activate the enzyme responsible for the production of AIs. Since the AI themselves are responsible for the production of more AIs, this loop is called a 'feed-forward' mechanism. On scaling up the production of AIs, they also activate various other genes that aid in biofilm formation like the EPS layer production. Gram-negative organisms produce acyl-homoserine lactones (AHL) with varying number of aliphatic chains and gram-positive organisms produce auto-inducer peptides (AIPs) as their autoinducers (4). The gene product of *icaADBC* is a polysaccharide intracellular adhesin in gram-positive bacteria like *Staphylococcus*, which expresses itself to mediate cell-to-cell adhesion and control the formation of biofilms (5). Their muco-polysaccharide-containing slime layer allows them to stick to surfaces and medical equipment, making it easy for them to colonize and proliferate throughout a hospital setting. Additionally, the slime factor contributes to their pathogenicity by shielding them from antimicrobial agents, phagocytosis, and chemotaxis (6). Antimicrobial resistance of biofilm forming bacteria can be up to 1000 times stronger than those of planktonic forms, and it is frequently imparted by multifactorial resistance mechanisms. This makes it extremely difficult to eliminate biofilm forming bacteria once they are established (7). Hence, there is an urgent need to find measures by which bacterial biofilms can be inhibited or disrupted, further solving the issue of drug resistance among many strains (2). Secondary metabolites present in several plants have been found to exhibit antibiofilm, antibacterial, and anti-quorum properties and therefore seem to be promising tools to deal with the menace of drug resistance (8). Silver nanoparticles (AgNPs) were shown to possess authentic characteristics and remarkable potential for the creation of new antimicrobial agents, drug delivery systems, coatings for biomaterials and medical devices, plat-

forms for detection and diagnosis of toxins, and therapeutic alternatives with improved performance (9). AgNPs are effective against a variety of cancers, including glioblastoma, colorectal adenocarcinoma, prostate carcinoma, cervical cancer, hepatocellular carcinoma, nasopharyngeal carcinoma, breast cancer and lung cancer. By damaging the ultrastructure of cancer cells, producing reactive oxygen species (ROS) and DNA damage, deactivating enzymes, and controlling signalling pathways, AgNPs can induce apoptosis or necrosis. Additionally, they also prevent angiogenesis and can thereby prevent the invasion and spread of malignant cells (10). The efficacy of silver nanoparticles in wound healing is greatly studied as they can prevent the colonization of bacteria and the development of biofilms if used in the early stages. From the previous literature, it has been deduced that a total of 6% of biopsy specimens from acute wounds and 60% of specimens from chronic wounds have biofilms detected in them. The microorganisms within biofilms provide the biggest obstacles to healing because they are resistant to various tolerance mechanisms and traditional antimicrobial therapy (1). AgNPs work against biofilms by either destroying the intermolecular interactions or stopping bacterial cells from sticking to surfaces. Additionally, it was demonstrated that AgNPs might prevent quorum sensing (11).

The present study attempts to check the antibiofilm efficacy of the plant extracts and nanoparticles of *P. guajava* and *S. jambos*, to formulate a gel from these plant extracts and test on human cell lines for possible use as a topical agent on wounds.

## Materials and Methods

### Bacterial isolates

*Chromobacterium violaceum* (MTCC 2656), *K. pneumoniae* (MTCC 109), *Pseudomonas aeruginosa* (MTCC 741) and *S. aureus* (MTCC 87)

### Sample collection and extraction

Leaves of *P. guajava* and *S. jambos* were collected from Trichur district in Kerala, India and shade dried for 14 days. Thereafter, the leaves were powdered using a blender into fine powder and 5 g of powder was used for Soxhlet extraction using 150 mL of ethanol.

### Antibacterial activity using agar well diffusion technique

100  $\mu$ L of overnight cultures of *P. aeruginosa*, *K. pneumoniae*, and *S. aureus* were spread plated on Mueller-Hinton agar and wells were made with a cork borer. 200  $\mu$ L of standard antibiotic (streptomycin sulphate-50  $\mu$ g/mL), ethanol, ethanolic extract of *P. guajava*, ethanolic extract of *S. jambos* (10 mg/mL), AgNPs (8 mg/mL) synthesized from *P. guajava*, AgNPs synthesized from *S. jambos*, and 1mm AgNO<sub>3</sub> were added into the wells. The plates were incubated overnight in a static incubator at 37°C in an upright position and observed for a zone of inhibition the next day (12). The experiment was done in triplicates and the mean value was given as the antibacterial activity.

### Phenotypic characterization of biofilm production in Congo Red Agar (CRA)

Congo Red Agar comprises Brain Heart Infusion broth, Sucrose, Congo red and Agar at 37 g/L, 5 g/L, 0.8 g/L and 15 g/L respectively. Congo Red stain was prepared as a concentrated solution and autoclaved separately. The stain was added to the remaining media at 55°C just before pouring the media into the plates. After solidifying the media, the cultures were quadrant streaked, and the plates were incubated at 37°C overnight. The formation of black coloured colonies with a crystalline appearance was inferred to be a positive result for biofilm production. The assay was done both in the presence and absence of plant extracts. In the case of media with plant extract, the test plant sample extracts were mixed with the media at a concentration of 10 mg/mL, before it solidified (13).

### Antibiofilm activity using Crystal Violet (CV) assay

Overnight cultures of *C. violaceum*, *P. aeruginosa*, *K. pneumoniae*, and *S. aureus* grown in Luria-Bertani (LB) broth were adjusted to 0.5 OD at 600 nm and 1 mL of these cultures were transferred to sterile test tubes in triplicates. 1 mL of ethanolic extract of *P. guajava* and *S. jambos* were added to the tubes. The tubes without the extracts served as controls while three tubes with sterile LB broth were treated as blanks. Cell suspensions were removed from the test tubes after 72 h. Tubes were washed with sterile distilled water and dried at 60°C for 30 min. Further, 1% Crystal Violet (CV) solution was added to all the tubes and incubated on a rocker for 30 min at room temperature. The tubes were cleared of the non-bound dye with repeated sterile distilled water wash following which tubes were dried at 37°C. 20% acetone was added to ethanol to dissolve the bound CV and incubated on a rocker for 15 min. Finally, to quantify the biofilms formed in the presence and absence of the extracts, the absorbance was measured at 600 nm (14). Uninoculated LB broth served as the blank.

### Screening of plant extracts for anti-quorum sensing (QS) activity against *C. violaceum*

Standard antibiotic (25 µg/mL), ethanol, the two plant extracts at 10 mg/mL concentration (individually and in combination), AgNPs synthesized from the plant extracts at 8 mg/mL concentration, and 1mM AgNO<sub>3</sub> were tested for their ability to prevent the formation of violacein in the strain *C. violaceum* (MTCC 2656) as described earlier with a few modifications. Briefly, 100 µL of the overnight culture of *C. violaceum* (MTCC 2656) was standardized to 0.5 OD at 600 nm and combined with 3 mL of melted LB agar (0.5% w/v agar). After that, the LB agar plate was layered with this mixture and allowed to solidify. Wells were bored with a cork-borer to hold 200 µL of the test samples. The plates were further incubated at 30°C overnight and the zone of inhibition of violacein production/growth was measured the following day (15).

### Quantitative estimation of violacein

Overnight culture of *C. violaceum* standardized to 0.5 OD at 600 nm and was grown in the absence and presence of

varying concentrations (10 mg/mL, 5 mg/mL, 2.5 mg/mL, 1.25 mg/mL, 0.62 mg/mL, 0.31 mg/mL and 0.15 mg/mL) of ethanolic leaf extracts of *P. guajava* and *S. jambos* respectively in LB broth. The tubes were incubated at 30°C in an orbital incubator at 220 rpm overnight. Following incubation, centrifugation was used to remove the insoluble violacein at 10000 rpm for 10 min. The pellet was gathered and then suspended in 1 mL of dimethyl sulfoxide (DMSO). The tubes were cyclo-mixed for 30 sec followed by centrifugation at 10000 rpm for 10 min for the removal of bacterial cells. Absorbance was recorded at 585 nm using a spectrophotometer to infer the amount of soluble violacein present in the supernatant (15).

### Minimum inhibitory concentration (MIC) assay

The minimum inhibitory concentration (MIC) of the test plant extracts was determined using the rapid INT (p-iodonitrotetrazolium chloride) colorimetric assay. It is a dye that changes its colour from yellow to pink when bacteria reduce it. The plant samples and the standard antibiotic were suspended in DMSO/Mueller Hinton broth such that the final concentration of DMSO was less than 2.5%. The obtained solution was added to Mueller Hinton broth and serially diluted to two folds along the columns of a 96 well plate. The stock concentration of the test samples was 10 mg/mL and they were diluted up to 3.12 mg/mL. The cultures were standardized to 0.5 OD and 100 µL of the standardized cultures were transferred to each well. Inoculated Mueller-Hinton broth with DMSO served as the negative control. The plate was closed with a lid and sealed before placing it on a plate shaker to mix the contents in the wells. Further, at 37°C, the plates were incubated for 18 h. Post incubation, each well was filled with 40 µL of 0.2 mg/mL INT, and the wells were incubated for 30 min at 37°C. In the wells in which bacterial growth was inhibited, the dye was not reduced, and they appeared pale yellow in colour whereas the ones that had bacterial growth showed a pink colour (16).

### Minimum bactericidal concentration (MBC) assay

After the MIC was deduced, from the wells that did not show a colour change in the MIC assay, the samples were added to 150 µL adequate broth and incubated at 37°C for 48 h in a new 96 well plate. The lowest concentration at which the wells did not show a colour change on addition of INT post incubation, was recorded as the MBC of that sample (16).

### Bacterial adherence to hydrocarbons (BATH) assay

The four isolates were harvested after 18 h of incubation and washed three times to further resuspend in 0.1M phosphate buffer (pH 7). 3 mL of the bacterial suspension was set to 0.8 OD at 550 nm using a spectrophotometer and was taken in a test tube to make them interact with 400 µL of a hydrocarbon, xylene. The solution was equilibrated at 25°C in a water bath for ten min and subsequently vortexed. The solution was left undisturbed for 15 min for the phase separation to happen such that the lower aqueous phase could be taken out to record the absorbance at 550 nm (A<sub>x</sub>). The readings were then compared to the con-

trol tubes wherein there was no interaction with the hydrocarbon. To infer the percentage of affinity that microbes have towards the hydrocarbon, the following formula was used:  $A = [(A_0 - A_1/A_0)] \times 100$  wherein;  $A_0$  is the absorbance of the control at 550 nm and  $A_1$  is the absorbance of the aqueous phase after the interaction of microbes with the hydrocarbon. The experiment was done in triplicates and the results were expressed as mean  $\pm$  standard deviation. The isolates were considered to be extremely hydrophobic if the percentage adhesion was more than 50%, intermediate when in the range of 20% to 50% and hydrophilic when below 20% (17). In an earlier study, bacterial isolates were isolated from the oral cavity of volunteers. These isolates are responsible for dental plaques and showed great adherence to hydrocarbons indicating their biofilm forming nature (18).

### Green synthesis of silver nanoparticles

20 mL of 1 mM  $\text{AgNO}_3$  solution was treated with 0.2 mL of leaf extracts to synthesize the AgNPs, which were then agitated for ten min at 30°C. A reddish brown colour gradually replaced the solution's initial pale-yellow appearance that indicated the presence of AgNPs (19).

### Characterization of AgNPs using UV-Vis spectrophotometer, scanning electron microscopy (SEM), X-ray diffraction (XRD) and energy dispersive X-ray (EDS) analysis

The surface plasmon resonance (SPR) of the noble metal AgNPs gives rise to their distinctive visual characteristics. GENESYS-180 UV-Visible spectrophotometer was used to perform UV-visible spectroscopy analyses of both the samples in the 350–700 nm range. Double-distilled deionized water was utilized as the blank for baseline correction (19). The size, morphology and weight of the synthesized AgNPs was investigated using Scanning Electron Microscopy integrated with Energy Dispersive X-Ray analysis using Zeiss Ultra 55. SEM was operated at a voltage of 5kV (20). Thin films of the synthesized nanoparticles were subjected to X-Ray Diffraction using Rigaku- Smartlab X-Ray Diffractometer.

### Formulation of gel

To make 50 mL of the gel, 2% Carbopol-934 was added to about 25 mL water and allowed to swell for two h. Further, the beaker with the carbopol mixture was kept on a magnetic stirrer for continuous agitation. Once the gelling agent was dispersed completely into the solution, 10 mL of the plant extract (10 mg/mL concentration) or the freshly synthesized nanoparticle solution was added and stirred for 18 h. 5 mL of glycerol was added to make the gel homogenous and finally an additional 10 mL of water was added to attain the 50 mL volume. pH was set to  $6.5 \pm 0.2$ . The gels were evaluated according to their physical characteristics namely: pH, grittiness, colour and spreadability (21).

### 3-(4,5-dimethylthiazol-2-yl)-2,5-diphenyltetrazolium bromide (MTT) assay

To test the toxicity of the synthesized gels, MTT assay was done using L-929 mouse fibroblast cell line procured from

NCCS, Pune. Following trypsinization, the cells cultured in a T-25 flask were aspirated into a 5 mL centrifuge tube and centrifuged at  $300 \times g$ . The pellet obtained was diluted using DMEM-HG medium to get a cell count of 10000 per 200  $\mu\text{L}$ . Every well in the 96 well plate was loaded with 200  $\mu\text{L}$  of cell suspension and incubated at 37°C and 5%  $\text{CO}_2$  atmosphere for 24 h. Post incubation, the consumed medium was aspirated and 200  $\mu\text{L}$  of test concentrations (31.25  $\mu\text{g/mL}$ , 62.5  $\mu\text{g/mL}$ , 125  $\mu\text{g/mL}$ , 250  $\mu\text{g/mL}$ , 500  $\mu\text{g/mL}$  and 1000  $\mu\text{g/mL}$ ) of the gels were added to the respective wells and incubated once again at 37°C and 5%  $\text{CO}_2$  atmosphere for 24 h. The drug containing media was aspirated following incubation and each well received 200  $\mu\text{L}$  of medium containing 10% MTT, resulting in a final concentration of 0.5 mg/mL. The plate was then incubated at 37°C and 5%  $\text{CO}_2$  atmosphere for 3 h. Without affecting the formazan crystals that had formed, the culture media was carefully removed. The crystals were subsequently solubilized in 100  $\mu\text{L}$  of DMSO and shaken gently using a gyratory shaker. The absorbance was read at 570 and 630 nm using a microplate reader (BK-EL10A, Biobase, China) to calculate the percentage growth inhibition of the fibroblast cells (22).

### Wound healing assay

L-929 mouse fibroblast cells were grown in a 12 well plate as a monolayer. Once 80% confluence was reached, a scratch was made on the cells to create a wound. The monolayer was washed twice with 1 mL DPBS following which 1 mL of medium with and without the drugs were added into the wells and incubated for 12 h. The gels were tested at a concentration of 250  $\mu\text{g/mL}$ . Images were taken at 0h and 12h using inverted phase contrast microscope (XDFL series, Sunny instruments, China). Percentage of cell migration is calculated by comparing the final gap area to the initial gap area using MRI Wound healing tool plug in ImageJ software (23).

## Results and Discussion

### Antibacterial activity using agar well diffusion technique

With a view to check the antibacterial activity of the ethanolic leaf extracts of *P. guajava* and *S. jambos*, four bacterial strains were used for the tests. These isolates were tested against the standard antibiotic (Streptomycin- 50  $\mu\text{g/mL}$ ), ethanol, ethanolic extract of *P. guajava*, ethanolic extract of *S. jambos*, a combination of both the extracts, AgNPs synthesized from *P. guajava* and *S. jambos* individually and 1mm  $\text{AgNO}_3$  respectively. A synergistic use of plant extracts against the four isolates proved to be slightly more potent than the single extracts (Table 1). The AgNPs synthesized from the two plant extracts however did not show better results than the plant extracts although a small zone of inhibition was observed (Fig 1). A two-way ANOVA was done to prove the statistical significance of the test. On obtaining a p value of  $<0.05$  a post hoc test named Tukey's Honestly Significant Test (HSD) was done which showed significant difference between



**Table 1.** Antibacterial activity of ethanolic leaf extracts of *Psidium guajava* and *Syzygium jambos*, against the biofilm forming bacterial isolates - *Chromobacterium violaceum*, *Klebsiella pneumoniae*, *Pseudomonas aeruginosa* and *Staphylococcus aureus*

Bacterial isolates	Zone of inhibition (mm)							
	Antibiotic (50 µg/mL)	Ethanol	Ethanolic extract of <i>P. guajava</i>	Ethanolic extract of <i>S. jambos</i>	<i>P. guajava</i> + <i>S. jambos</i>	AgNPs synthesized from <i>P. guajava</i>	AgNPs synthesized from <i>S. jambos</i>	1 mM AgNO <sub>3</sub>
<i>C. violaceum</i>	45	15	22	23	21	15	16	15
<i>K. pneumoniae</i>	33	10	16	20	28	11	11	10
<i>P. aeruginosa</i>	40	15	18	21	25	14	14	10
<i>S. aureus</i>	32	10	18	21	23	12	13	12

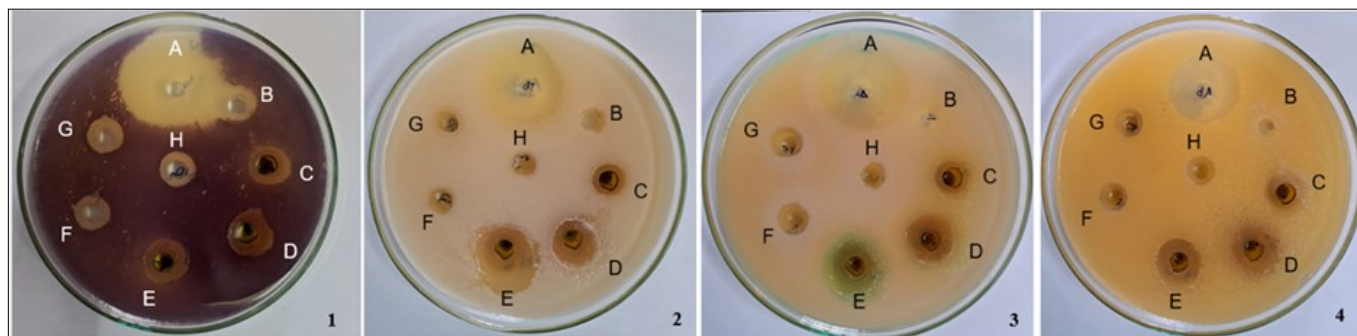


**Fig. 1.** Sensitivity patterns of the 4 isolates (1-*Chromobacterium violaceum*, 2-*Klebsiella pneumoniae*, 3-*Pseudomonas aeruginosa*, 4-*Staphylococcus aureus*) grown on Mueller-Hinton Agar against A-Std Antibiotic Streptomycin (50µg/mL), B-Ethanol, C-Ethanolic Leaf Extract of *Psidium guajava*, D-Ethanolic Leaf Extract of *Syzygium jambos*, E- Plant Extracts in Combination, F-AgNPs Synthesized from *Psidium guajava*, G-AgNPs Synthesized from *Syzygium jambos*, H-1mM Silver Nitrate.

specific samples used for the assay. In an earlier study conducted by Yahaya *et al.*, ethanolic leaf extract of guava showed good antibacterial activity against test organism at concentration of 200 mg/mL with a zone of inhibition of 16 mm. In the current study, ethanolic leaf extract of *P. guajava* showed better results at much lesser concentration of 10 mg/mL with a zone of inhibition of 22 mm, 16 mm, 18 mm and 18 mm against *C. violaceum*, *K. pneumoniae*, *P. aeruginosa* and *S. aureus* respectively (24). The ethanolic extracts of *P. guajava* and the methanolic extract of *S. jambos* showed significant antibacterial activity against the *B. anthracis* 34F2 Sterne strains with a MIC value of 64 µg/mL. This significant antibacterial activity of plants could be attributed to the presence of vanillic acid in both extracts. Vanillic acid disrupts the cell membrane leading to bacterial cell death (25). The results of these studies align with

the current study and reiterate the presence of bioactive compounds in the extract that contribute towards the antibacterial activity.

#### Phenotypic characterization of biofilm production in Congo Red Agar (CRA)

All four isolates exhibited luxuriant growth on CRA plates without plant extracts. They also showed black colour or close to black colour colonies indicating the presence of biofilms after 24-48 h of incubation at 37°C. Fig. 2 depicts the growth of *S. aureus* on Congo Red Agar with and without plant extracts. *P. aeruginosa* and *C. violaceum* are pigment producing organisms and therefore the colour of the colonies on CRA appeared purplish black and greyish black for these isolates respectively (Fig. S1). The precise mechanism of the reaction involved in the Congo Red Agar test is unknown, despite the fact that it is frequently uti-

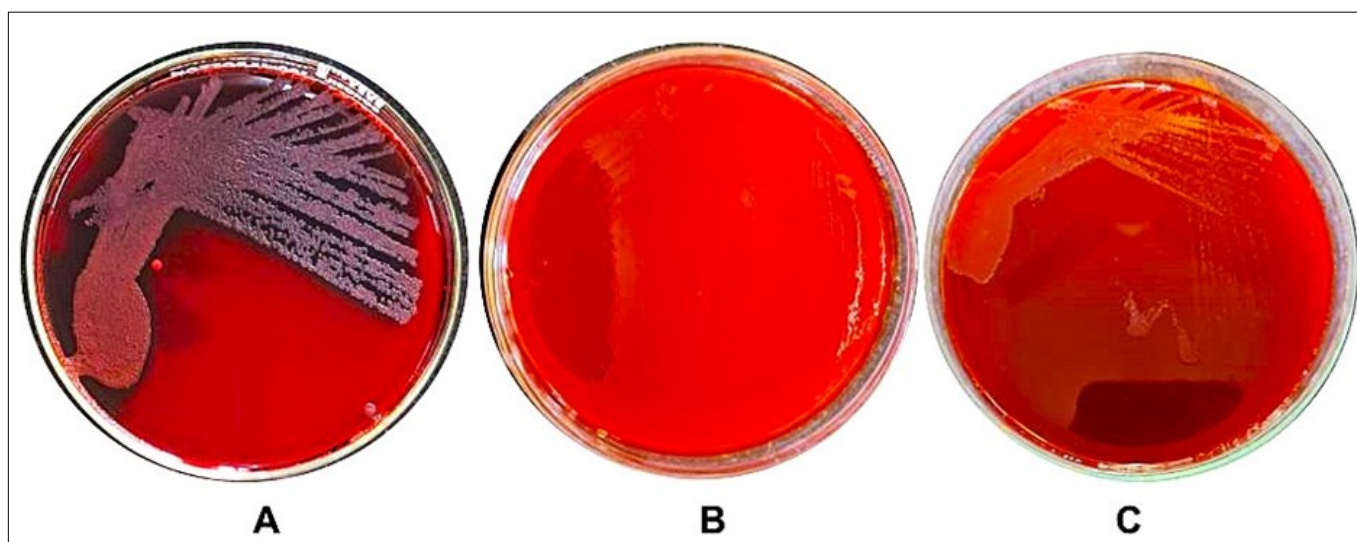


**Fig. 2.** *Staphylococcus aureus* isolate grown on Congo Red Agar. A - Control, with no extract added, B - Media with ethanolic extract of *Syzygium jambos* and C - Media with ethanolic extract of *Psidium guajava*.

lized in biofilm investigations, primarily involving *Staphylococcus* spp. (26). Furthermore, there have been reports of changes in the composition of biofilms across different species of bacteria and it is believed that these variations in Exopolysaccharide (EPS) production are the reasons for the variations in the positive colour tone detected by the Congo Red Agar Method (27). Black colonies produced by the reaction of Congo Red with beta glucans in the exopolysaccharide, aid in the differentiation of EPS producers from non-EPS producers (28). However, this qualitative approach of identifying the isolates based on whether they are biofilm formers or not is not something that is 100% reliable. Quantitative methods like the Crystal Violet assay and molecular techniques need to be used (5).

#### Antibiofilm activity of ethanolic leaf extract of *P. guajava* and *S. jambos* using Crystal Violet (CV) assay

A common method for assessing the earliest phases of bacterial biofilm development is the crystal violet-based test (29). It is inexpensive and does not require any sophisticated instrument and therefore one of the primary tests done to evaluate the capability of the bacterial strains to establish biofilms. Here, in the current study, the four bacterial isolates were compared based on their ability to form biofilms in the presence and absence of the plant extracts. Among the 4 strains, *P. aeruginosa* gave the maximum OD readings (2.822) in the absence of the plant extracts followed by *S. aureus* (2.19), *C. violaceum* (1.13) and *K. pneumoniae* (1.06). In the presence of ethanolic leaf extract of *S. jambos*, all four isolates showed inhibition of biofilms largely, followed by the two plant extracts in com-

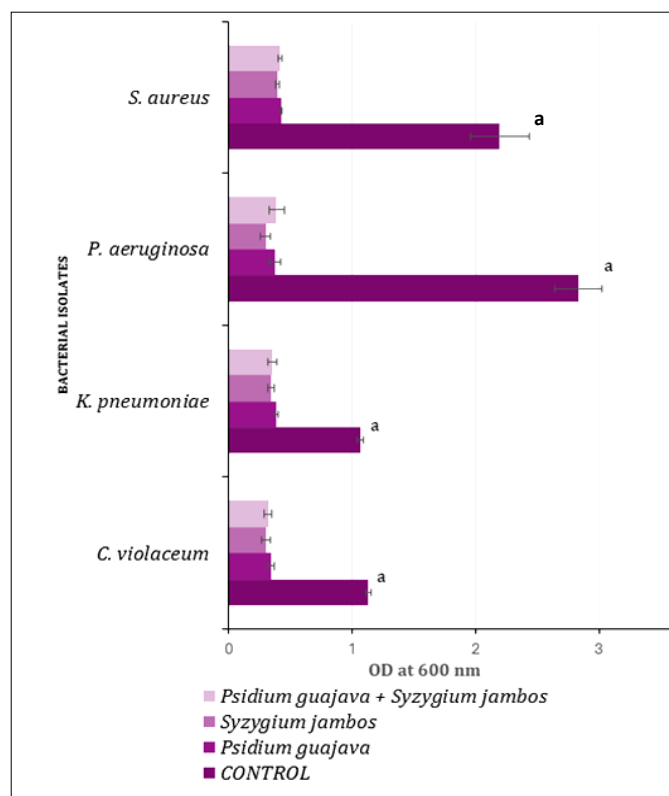


**Fig. 3.** Biofilm formation and prevention in *Chromobacterium violaceum*, *Klebsiella pneumoniae*, *Pseudomonas aeruginosa* and *Staphylococcus aureus* when treated with ethanolic leaf extracts of *Psidium guajava* and *Syzygium jambos*. The values are represented as means of three independent determinations and control samples are marked with superscript a, indicating that the values are significantly different from the treated samples using one way

bination and ethanolic leaf extract of *P. guajava* respectively. The extent of biofilm reduction across the treatment groups has been represented in Fig. 3. The values are represented as means of three independent determinations and control samples are marked with superscript a, indicating that the values are significantly different from the treated samples using one way ANOVA, Duncan,  $p < 0.05$  in SPSS software. Error bars depict mean  $\pm$  standard deviation.

#### Screening of plant extract for anti-QS activity against *C. violaceum*

Quorum sensing is a phenomenon that happens in a few classes of bacteria to communicate with each other via signalling molecules called autoinducers to execute a task. These tasks include secretion of toxins, metalloproteases, lipases, collagenases, chitinases, formation of biofilm, to exhibit bioluminescence property, pigment production etc. In *C. violaceum* there are two genes that are crucial in the QS system viz. *CviI* and *CviR*. These are homologous to *LuxI* and *LuxR* that respond with a high affinity to acyl homoserine lactones that act as signalling molecules for the increase in population density. *CviI* AHL synthase is an enzyme that facilitates the synthesis of *N*-decanoyl-L-homoserine lactone, which is a signalling molecule, and *CviR*, codes for a transcriptional regulatory protein (30). When the population size increases, the AHL molecules bind to the respective receptors to form a complex that regulates the target genes. In *C. violaceum*, violacein production and eventually biofilm formation is regulated by the target operon *vioABCDE*. Any molecule that can block these interactions can prevent pigment production and biofilm formation in *C. violaceum* and can therefore be called quorum sensing inhibitors (QSIs). Among the various samples used against *C. violaceum*, the ethanolic leaf extract of *S. jambos* showed the maximum level of pigment inhibition (6 mm) followed by a combination of ethanolic leaf extracts of *P. guajava* and *S. jambos* (5 mm) as depicted

**Table 2.** Quorum sensing inhibition in *C. violaceum* when treated with potential quorum sensing inhibitors

Samples	Zone of inhibition against <i>C. violaceum</i>		
	Growth + Pigment inhibition or Total inhibition ( $d_1$ )	Growth inhibition ( $d_2$ )	QS inhibition ( $d_1 - d_2$ )
Ethanol	15	13	2
Ethanolic leaf extract of <i>P. guajava</i>	17	15	2
Ethanolic leaf extract of <i>S. jambos</i>	24	16	6
Extracts of <i>P. guajava</i> and <i>S. jambos</i>	19	14	5
AgNPs synthesized from <i>P. guajava</i>	19	19	Nil
AgNPs synthesized from <i>S. jambos</i>	21	21	Nil
Silver Nitrate	18	18	Nil

ed in Table 2. The inhibition of pigment production using

the plant extract is clearly observed in Fig. 4.

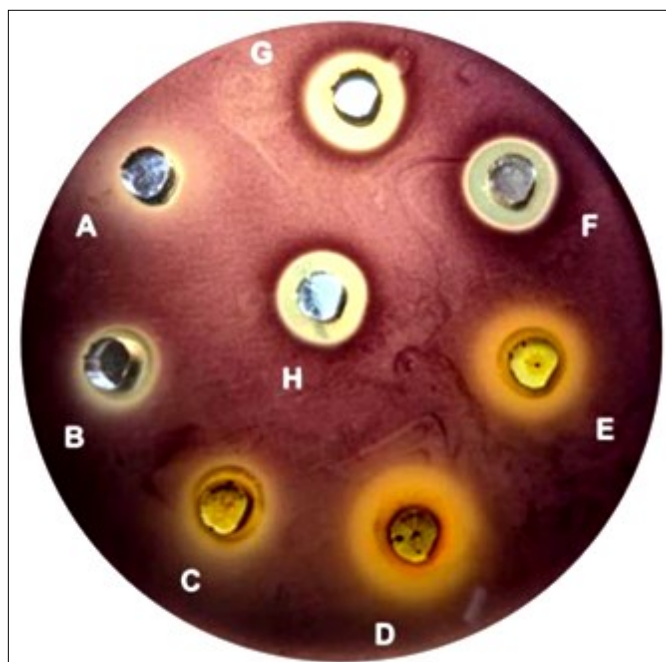


**Fig. 4.** Anti-quorum activity of **A**-Streptomycin (25µg/mL), **B**-Ethanol, **C**- Ethanolic leaf extract of *Psidium guajava*, **D**- Ethanolic leaf extract of *Syzygium jambos*, **E**-Combination of the two plant extracts, **F**-AGNPs synthesized from *Psidium guajava*, **G**- AGNPs synthesized from *Syzygium jambos*, and **H**-1mM AgNO<sub>3</sub> against *Chromobacterium violaceum* grown in Luria Bertani Agar (LBA).

### Quantitative estimation of violacein

On treating the bacterial isolate with the two different plant extracts, the inhibition of violacein in *C. violaceum* happened in a dose dependent manner with 10 mg/mL of

both *P. guajava* (74.70%) and *S. jambos* (78.84%) showing the highest inhibition (Fig. 5). The percentage inhibition was calculated by using the untreated isolate as the reference standard. In comparison, *S. jambos* showed slightly better results. Higher concentration of the extract barely showed any colour (Fig. S2). In an earlier study that used aqueous extract of guava leaves, inhibition of violacein pigment production of 85% was observed at a concentration of 400 µg/mL which was comparatively better than the results obtained in the current study with ethanolic leaf extracts (31). In another study, at 0.5 mg/mL, extracts of *S. cumini* and *P. dioica* demonstrated over 80% inhibition of violacein synthesis, and at 1.0 mg/mL, it demonstrated total inhibition. However, both plant samples from the Myrtaceae family were pure forms of the extracts and probably the reason for its high potential anti-quorum activity (32).

### Determination of MIC and MBC values

All four isolates showed susceptibility to the plant extracts at 5 mg/mL concentration. Among them *K. pneumoniae* showed susceptibility at even lower concentration of 2.5 mg/mL. The MBC/MIC ratio for the plant extracts against all the isolates was calculated to be 2, indicating that the extracts are bactericidal in nature (33). The MIC values, MBC values and the MBC/MIC ratio are tabulated (Table 3) which gives an indication of whether the extracts are bacteriostatic or bactericidal.

### BATH assay

Hydrophobicity is essential for bacterial germs to adhere to surfaces. The repulsion between the bacterial cell sur-

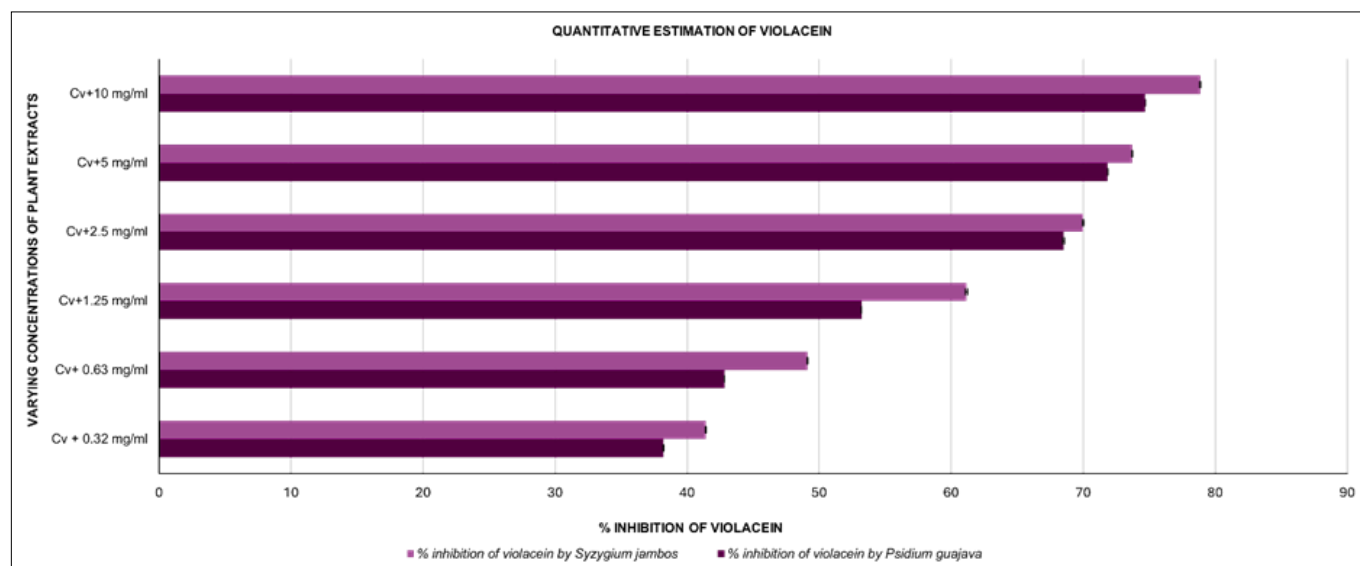


**Fig. 5.** Percentage inhibition of violacein in *Chromobacterium violaceum* in the presence of ethanolic leaf extracts of *Psidium guajava* and *Syzygium jambos*.

**Table 3.** MIC and MBC values of ethanolic leaf extracts of *P. guajava* and *S. jambos*

Bacterial isolates	Ethanolic leaf extract of <i>P. guajava</i>			Ethanolic leaf extract of <i>S. jambos</i>		
	MIC (mg/mL)	MIC (mg/mL)	MBC/MIC ratio	MIC (mg/mL)	MBC (mg/mL)	MBC/MIC ratio
<i>C. violaceum</i>	5	10	2	5	10	2
<i>K. pneumoniae</i>	2.5	5	2	2.5	5	2
<i>P. aeruginosa</i>	5	10	2	5	10	2
<i>S. aureus</i>	5	10	2	5	10	2



face and the substrate is lessened by the hydrophobic effect, which makes a hydrophobic surface more favourable for bacterial colonization than a hydrophilic one (34). Among the four isolates that were used for BATH assay, *P. aeruginosa* (73.37%) showed the highest percentage adherence towards hydrocarbon xylene, followed by *S. aureus* (50.5%), *C. violaceum* (41.5%) and *K. pneumoniae* (26.37%). represented in Fig. 6. According to previous literature, the isolates were considered to be extremely hydrophobic if the percentage adhesion was more than 50%, intermediate when in the range of 20%-50% and hydrophilic when below 20% and directly correlates with their ability to form biofilms (17) and therefore in the present study, both *P. aeruginosa* and *S. aureus* can be classified as extremely hydrophobic and *C. violaceum* and *K. pneumoniae* can be classified under the intermediate group. All isolates were significantly different from each other with respect to their percentage adherence to hydrocarbon xylene and the significance was proven using one-way ANO-

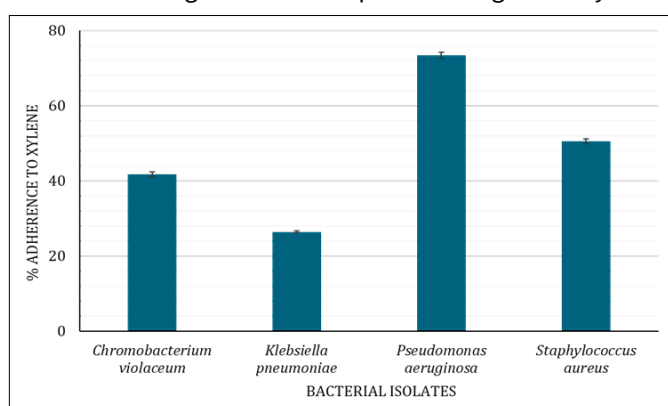


**Fig. 6.** Percentage Bacterial Adherence to Hydrocarbon- Xylene of bacterial isolates-*Chromobacterium violaceum*, *Klebsiella pneumoniae*, *Pseudomonas aeruginosa* and *Staphylococcus aureus*.

VA in SPSS software. The values are represented as means of three independent determinations and the error bars depict mean  $\pm$  standard deviation.

### Green synthesis of AgNPs

20 mL of 1mM silver nitrate and 200  $\mu$ L of each plant extract were used for the synthesis of AgNPs. After ten min of

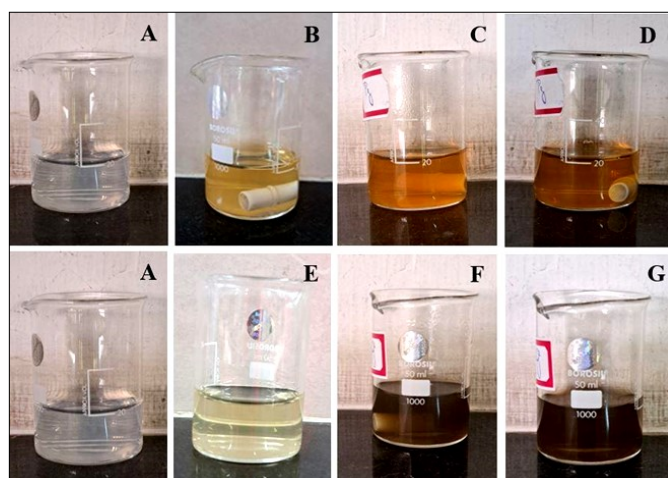


**Fig. 7.** Green synthesis of AgNPs from ethanolic leaf extracts of *Psidium guajava* and *Syzygium jambos*. **A:** 1 mM  $\text{AgNO}_3$ , **B:** 200  $\mu$ L ethanolic leaves extract of *Psidium guajava* + 20 mL 1 mM  $\text{AgNO}_3$  at 0 min, **C:** After 10 min incubation time **D:** After 30 min incubation time, **E:** 200  $\mu$ L ethanolic leaves extract of *Syzygium jambos* + 20 mL 1 mM  $\text{AgNO}_3$  at 0 min, **F:** After 10 min incubation time, **G:** After 30 min incubation time.

continuous stirring at 30°C, the colour of the solution turned from colourless to the colour of honey and the intensity of the colour increased after 30 min of incubation (Fig. 7). The stirring was stopped after a 30-min incubation period. This colour change is a characteristic feature of silver nanoparticle synthesis (19).

### Characterization of AgNPs using UV-Vis spectrophotometer, SEM-EDS and XRD

When subjected to UV Vis spectrophotometry, a peak was obtained at 418 nm for AgNPs synthesized from *P. guajava*

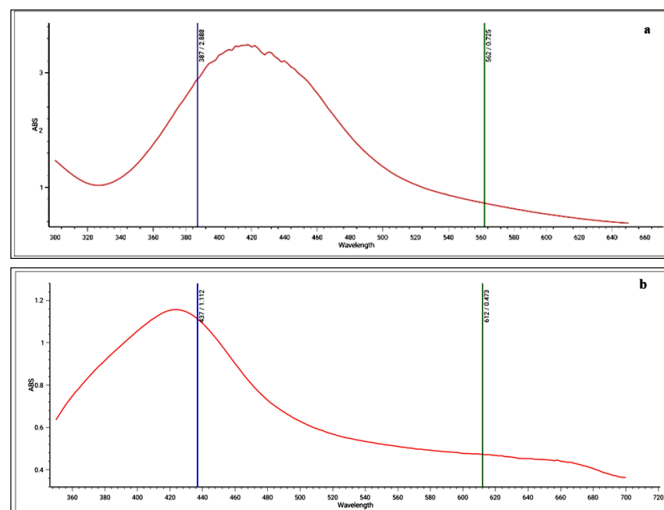


**Fig. 8.** UV-Vis peak for AgNPs synthesized from (a) *Psidium guajava* and (b) *Syzygium jambos* after 30 min of incubation in dark.

and at 424 nm for AgNPs synthesized from *S. jambos* with an absorbance of 3.48 and 1.156 respectively (Fig. 8a & b). These peaks are characteristic of AgNPs and the broadening of the peaks suggests that the particles were scattered widely (35). The nanoparticles synthesized from the plant extracts, when subjected to SEM analysis, appeared in the form of nanoflakes (Fig. 9a & 9c). The images show agglomerated nanoparticles synthesized from the two plant extracts. The nanoparticles synthesized from ethanolic leaf extracts of *P. guajava* and *S. jambos* showed an average particle size of 65.20 nm and 144.94 nm respectively. In the EDS graph, a strong peak was obtained at 3keV (Fig. 9b & 9d) which is characteristic of silver metal and showed a total weight of 22.36%. There were peaks that corresponded to other elements like Si, C, O, and Cl which might have originated from the biomolecules that the surface of Ag-NPs contained (36). The Debye-Scherrer equation,  $D = K\lambda/\beta \cos\theta$ , was used to determine the size of the silver nanoparticles where D is the crystallite size, K is the constant, which is equal to 0.94,  $\lambda$  is the wavelength of the X-ray,  $\beta$  is the full width half maximum of the peaks measured in radians, and  $\theta$  is the Bragg angle (37). On substituting the values in the formula, the crystallite size of the AgNPs synthesized from ethanolic extract of *P. guajava* and *S. jambos* were found to be 14.562 nm and 14.24 nm respectively. Several Bragg reflection peaks were observed at  $2\theta$  values of 27.8°, 32.4°, 38.1°, 44.31°, 46.23°, 54.7°, 57.28°, and 64.8° (Fig. 10) which are correlated to (210), (122), (111), (200), (231), (142), (241), and (220) for planes of silver synthesized from *P. guajava* and *S. jambos*.



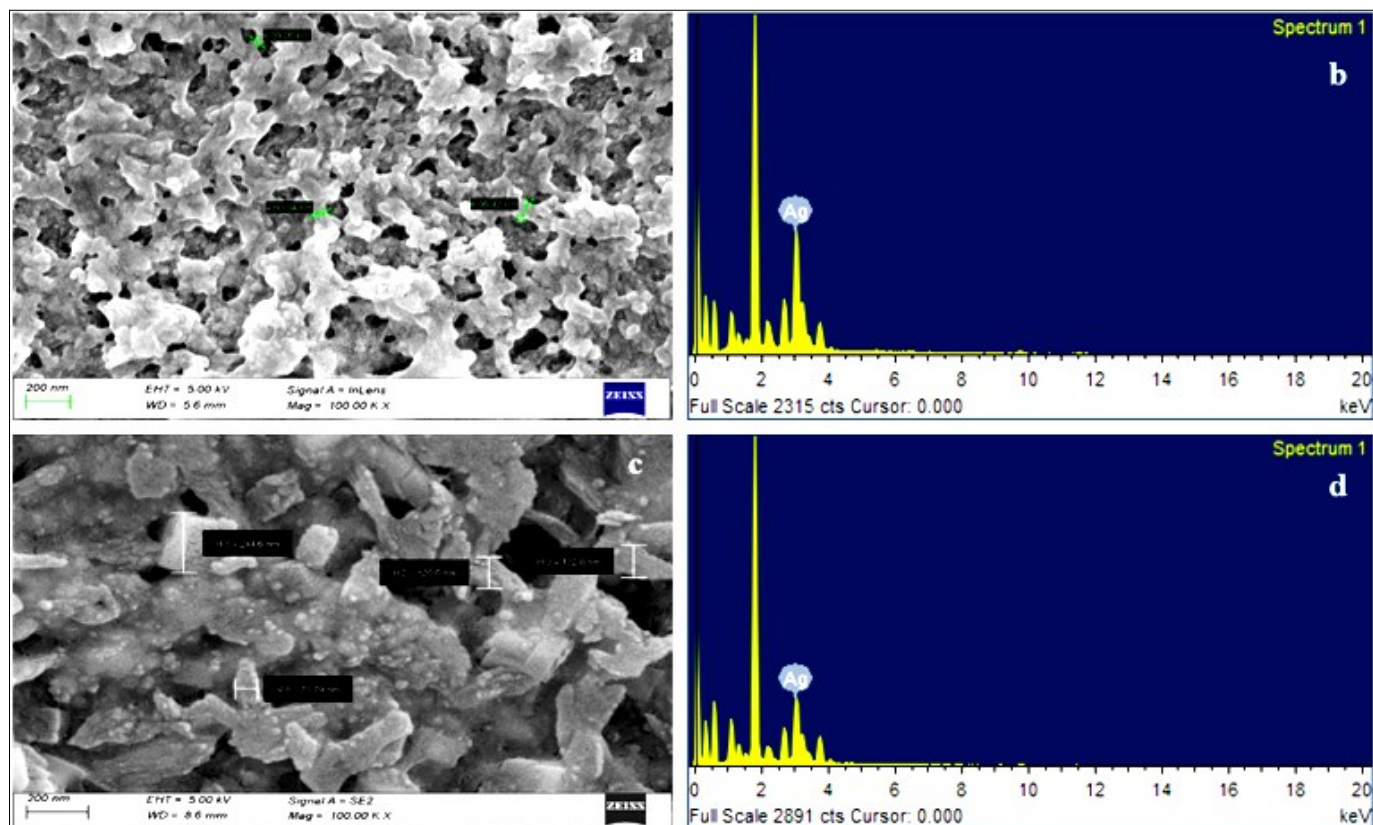


**Fig. 9.** Scanning electron Microscopy images of **A)** *Psidium guajava* and **(C)** *Syzygium jambos* and Energy Dispersive Spectrum analysis of AgNPs synthesized from **(B)** *Psidium guajava* and **(D)** *Syzygium jambos*.

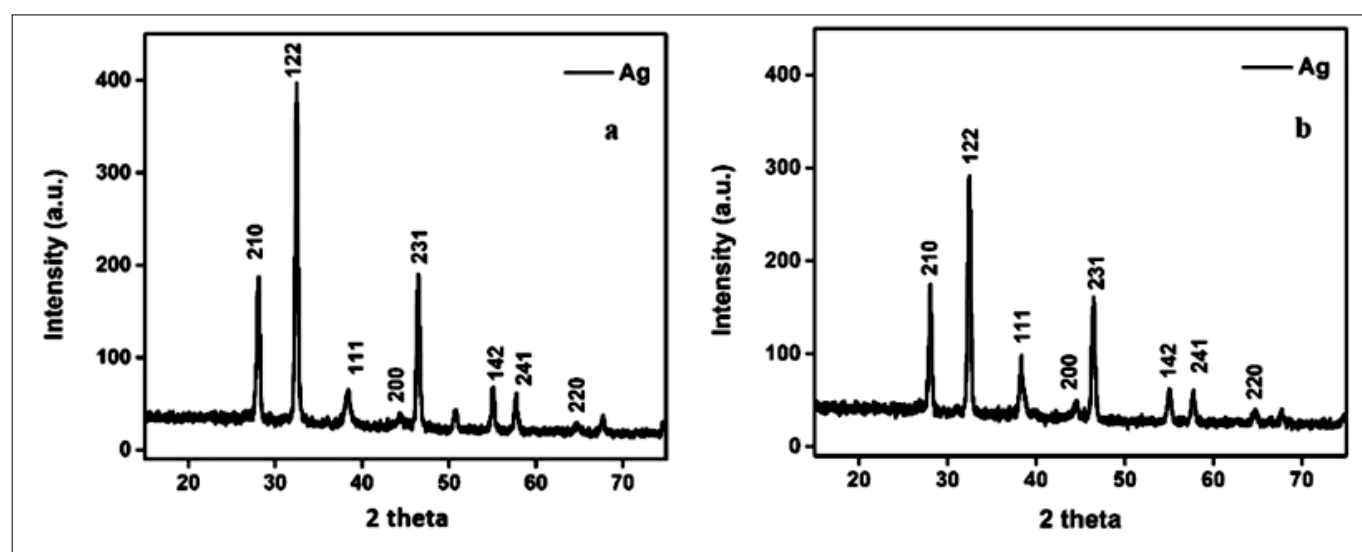


**Fig. 10.** XRD analysis of AgNPs synthesized from **(a)** *Psidium guajava* and **(b)** *Syzygium jambos*.

Although the synthesis of AgNP from plant extracts provides a "green" and environmentally friendly method, its scalability may be constrained by elements such as the variability of plant phytochemical composition, the difficulty of standardizing extraction procedures, and the possibility of difficulties in achieving consistent nanoparticle size and morphology across large-scale production. For this reason, it is important to optimize conditions for consistent quality control; additionally, the dependence on natural sources may result in supply chain problems due to seasonal fluctuations and plant availability.

#### Formulation of wound healing gel

Bacterial infections pose serious delays in wound healing. With a view to create a wound healing gel formulation,

plant extracts were mixed with various biocompatible ingredients. Five different gels were synthesized using Carbopol-934 and glycerol mixed with plant extracts and stored in glass bottles at 4°C for further analysis (Fig. 11). The gels were tested for various properties including pH, grittiness, colour and spreadability and the results are depicted in Table 4.

#### MTT assay

Although the physical properties of the gels were satisfactory, it was imperative to check the toxicity aspect before recommending it for application. MTT assay was done on L-929 mouse fibroblast cell line to test the toxicity of the synthesized gels. The cells were exposed to the gels in varying concentrations (31.25 µg/mL, 62.5 µg/mL, 125 µg/mL,

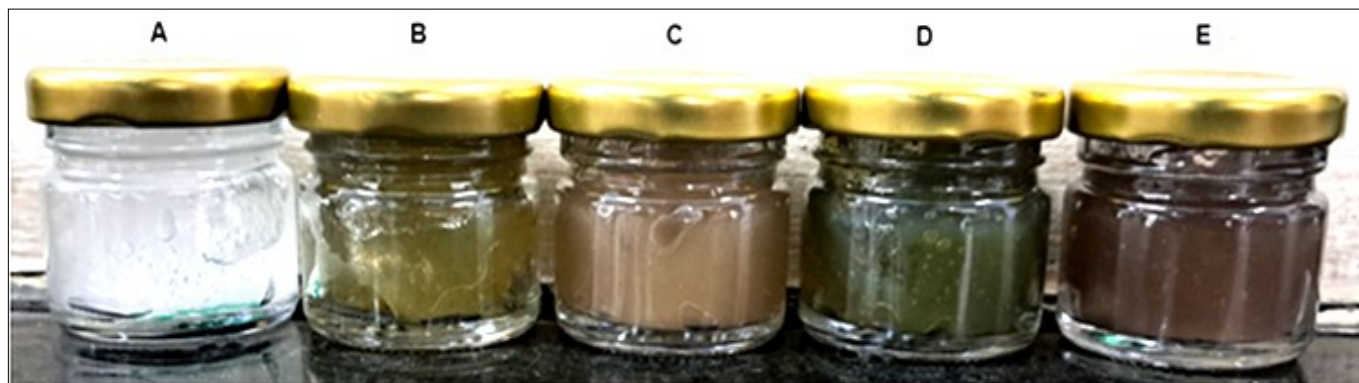


**Fig. 11.** A - Control, B - Gel with ethanolic leaf extract of *P. guajava*, C - Gel with silver nanoparticles synthesized from *P. guajava*, D - Gel with ethanolic leaf extract of *S. jambos*, E - Gel with silver nanoparticles synthesized from *S. jambos*.

**Table 4.** Evaluation of formulation of gels made using the extracts of *P. guajava* and *S. jambos* based on the physical and chemical properties

Gel	pH	Grittiness	Colour	Spreadability (sec)
Control	6.6	No	White	8
Gel synthesised with AgNPs from <i>P. guajava</i>	6.5	No	Brown	6
Gel synthesised with AgNPs from <i>P. guajava</i>	6.5	No	Light Green	7
Gel synthesized with AgNPs from <i>S. jambos</i>	6.6	No	Brown	6
Gel with ethanolic extract of <i>S. jambos</i>	6.6	No	Green	7

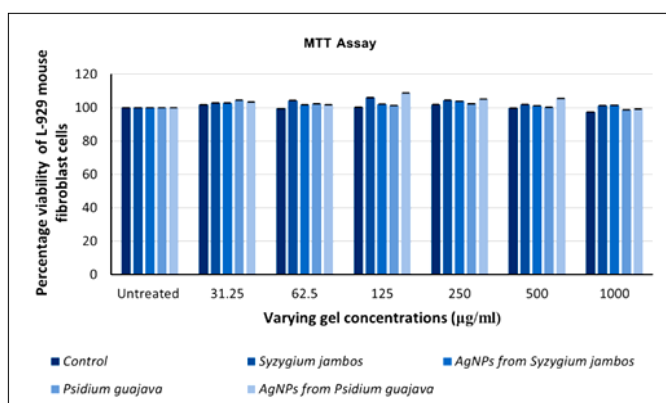


**Fig. 12.** Comparison of Percentage viability of L-929 mouse fibroblast cell line between untreated cell line and when exposed to the synthesized gels- Control, *Syzygium jambos*, AgNPs synthesized from *Syzygium jambos*, *Psidium guajava* and AgNPs synthesized from *Psidium guajava* in various concentrations. A two-way ANOVA was performed to check the statistical significance of the test using SPSS software. A p value > 0.05 was obtained (0.991) indicating that there is no significant difference between the treated and the untreated cell line.

250 µg/mL, 500 µg/mL, and 1000 µg/mL). The L-929 cells showed their characteristic morphology of spindle shape even after the exposure which proved that the gels are non-toxic and are safe to use. The percentage viability of the cells is given in the graphs represented in Fig. 12. A two-

way ANOVA was performed to check the statistical significance of the test using SPSS software. A p value > 0.05 was obtained (0.991) indicating that there is no significant difference between the treated and the untreated cell line, hence proving the non-toxic nature of the formulated gels.

### Wound healing assay

Numerous cell types and additional microenvironmental factors are involved in the three primary stages of fibroblast cell wound healing: activation, proliferation, and migration. The scratch assay is a commonly used *in vitro* method to investigate the potential for medicinally significant substances to heal wounds (23). In the current study, L-929 cells were treated with 5 different gels at concentration 250 µg/mL and compared them to the wound size in the untreated cells. The cells were monitored microscopically at 0 h and 12 h to observe the rate at which the wound closure occurs (Fig. 13). From the results it has been observed that the cells treated with gel that comprises of AgNPs from the ethanolic extract of *S. jambos* (89.14%) and the plant extract of *S. jambos* (85.77%) showed faster migration of cells and enclosure within a period of 12 h. The rate at which wound healing occurred

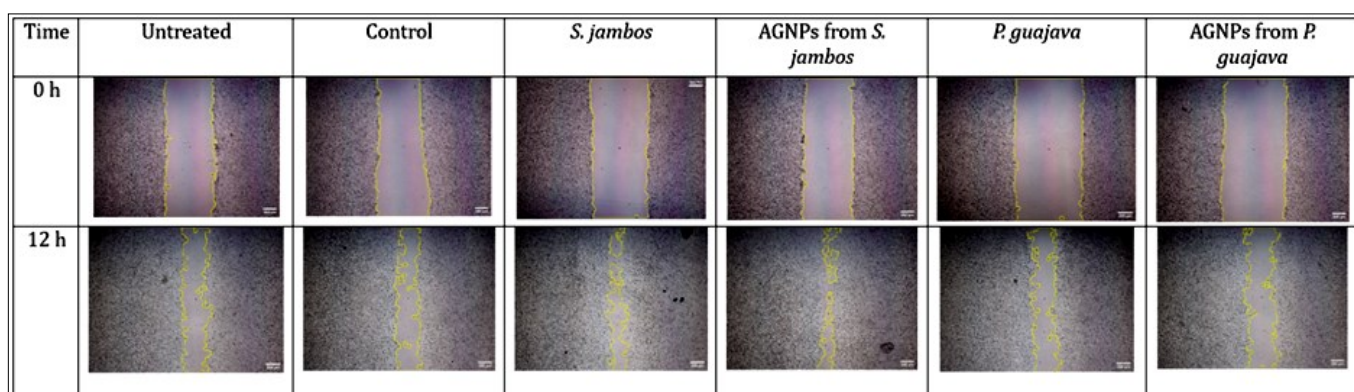


**Fig. 13.** Comparison of microscopic images of wound healing in L-929 Fibroblast cell line at 0 h and 12 h between Untreated Cell line and Cell lines exposed to Control gel, Gel with *Syzygium jambos* plant extract, Gel with AgNPs synthesized from *Syzygium jambos*, Gel with *Psidium guajava* plant extract, and Gel with AgNPs synthesized from *Psidium guajava*.

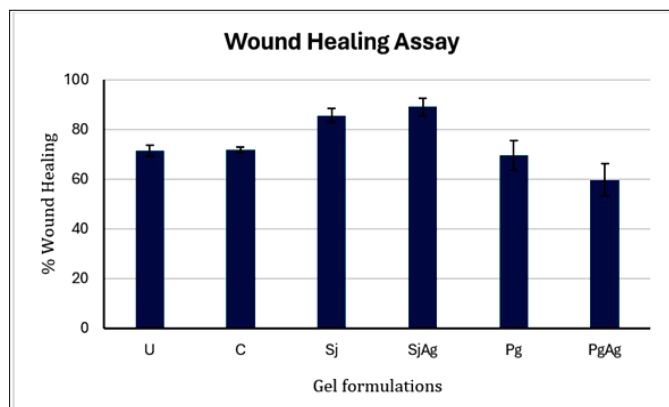


**Fig. 14.** Comparison of wound healing in L-929 fibroblast cell line at the end of 12 h between U: Untreated cell line and cell lines exposed to C: Control gel, Sj- Gel with *Syzygium jambos* plant extract, SjAg- Gel with AgNPs synthesized from *Syzygium jambos*, G: Gel with *Psidium guajava* plant extract and PgAg: Gel with AgNPs synthesized from *Psidium guajava*.

is represented in Fig. 14. A longer exposure time could have healed the wound completely in all the cases, indicating the high medicinal value of the synthesized gels. Aside from the potential advantages of using plant-based treatments in clinical - such as a decreased dependency on synthetic chemicals, more environmentally friendly practices, cost effectiveness, and access to natural remedies for specific conditions—there are drawbacks as well, such as issues with quality control, standardization, and the requirement for thorough scientific research to verify safety and efficacy.

## Conclusion

In conclusion, plants are a storehouse of phytochemicals with innumerable bioactive compounds and are currently the focus in the medical domain. The number of bacterial species that are acquiring resistance to a wide spectrum of antibiotics is growing at an alarming scale and hence it is imperative that we find a sustainable solution to this problem. Predominantly, the antibiotic resistance genes are transferred from one bacterium to the other via a method called horizontal gene transfer without a species barrier. Most importantly, the transfer is made possible when bacterial cells are in proximity like in the case of a biofilm. Specifically in a condition like wounds in diabetic patients, the bacterial cells are able to grow at an accelerating speed because of the excess blood sugar level. This allows them to establish their colony at the site and further aid in biofilm formation. Therefore, biofilm disrupting agents which can interfere with quorum sensing of bacteria are required to prevent biofilm related infections, gangrene and amputation. Hence, a timely medical intervention can be helpful in restricting the spread of infection. In the current study, the ethanolic leaf extracts of *P. guajava* and *S. jambos* have given good results with respect to their anti-biofilm properties against four dangerous biofilm forming bacterial pathogens. The gels formulated using the ethanolic leaf extract of *S. jambos* and the AgNPs synthesized from *S. jambos* showed excellent wound healing property which indicates its potential use as topical agents on acute and chronic wounds. However, currently only *in vitro* studies have been done and a much-detailed study is to be done on animal models to be sure of the non-toxic nature

and the efficacy of the synthesized gels against biofilm forming pathogens at wound sites. In contrast to *in vitro* research, which just looks at isolated cells or tissues, *in vivo* research provides crucial information about physiological reactions and possible side effects of a drug on the whole body that are impossible to record in a lab setting. A comprehensive study on the drug kinetics should also be performed for consistent results.

## Acknowledgements

The authors would like to acknowledge the continuous support provided by the Department of Life Sciences, CHRIST (Deemed to be University), Bengaluru, India.

## Authors' contributions

SS has conceptualized, supervised, reviewed, and edited. SKS did the methodology, software, investigation, and writing of the original draft.

## Compliance with ethical standards

**Conflict of interest:** The authors declare that no competing interest exists.

**Ethical issues:** None

## Supplementary data

Supplementary figures

Fig.S1: Bacterial isolates (A: *Chromobacterium violaceum* B: *Klebsiella pneumoniae* C: *Pseudomonas aeruginosa* D: *Staphylococcus aureus*) grown on Congo Red Agar (CRA)- control; 2-Bacterial isolates grown on CRA treated with ethanolic leaf extract of *Psidium guajava*; 3-Bacterial isolates grown on CRA treated with ethanolic leaf extract of *Syzygium jambos*

Fig.S2: *C. violaceum* incubated with varying concentrations of ethanolic leaf extracts of *Psidium guajava* and *Syzygium jambos*.

## References

- Paladini F, Pollini M. Antimicrobial silver nanoparticles for wound healing application: progress and future trends. *Materials (Basel)*. 2019;12(16):2540. <https://doi.org/10.3390/ma12162540>
- Dumar R, Baral R, Shrestha LB. Study of biofilm formation and antibiotic resistance pattern of gram-negative Bacilli among the clinical isolates at BPKIHS, Dharan. *BMC Res Notes*. 2019;12(1):38. <https://doi.org/10.1186/s13104-019-4084-8>
- Li J, Zhao X. Effects of quorum sensing on the biofilm formation and viable but non-culturable state. *Food Res Int*. 2020;137:109742. <https://doi.org/10.1016/j.foodres.2020.109742>
- Samrot AV, Mohamed A, Faradjeva E, Si JL, Hooi SC, Arif A, et al. Mechanisms and impact of biofilms and targeting of biofilms using bioactive compounds—A review. *Medicina (Kaunas)*. 2021;57(8):839. <https://doi.org/10.3390/medicina57080839>



5. Harika K, Shenoy VP, Narasimhaswamy N, Chawla K. Detection of biofilm production and its impact on antibiotic resistance profile of bacterial isolates from chronic wound infections. *J Glob Infect Dis.* 2020;12(3):129–34. [https://doi.org/10.4103/jgid.jgid\\_150\\_19](https://doi.org/10.4103/jgid.jgid_150_19)
6. Shrestha LB, Bhattarai NR, Khanal B. Antibiotic resistance and biofilm formation among coagulase-negative staphylococci isolated from clinical samples at a tertiary care hospital of eastern Nepal. *Antimicrob Resist Infect Control.* 2017;6(1):89. <https://doi.org/10.1186/s13756-017-0251-7>
7. Basnet A, Tamang B, Shrestha MR, Shrestha LB, Rai JR, Maharjan R, et al. Assessment of four in vitro phenotypic biofilm detection methods in relation to antimicrobial resistance in aerobic clinical bacterial isolates. *PLoS One.* 2023;18(11):e0294646. <https://doi.org/10.1371/journal.pone.0294646>
8. Khan MA, Celik I, Khan HM, Shahid M, Shahzad A, Kumar S, et al. Antibiofilm and anti-quorum sensing activity of *Psidium guajava* L. leaf extract: *In vitro* and *in silico* approach. *PLoS One.* 2023;18(12):e0295524. <https://doi.org/10.1371/journal.pone.0295524>
9. Burduşel AC, Gherasim O, Grumezescu AM, Mogoantă L, Ficai A, Andronescu E. Biomedical applications of silver nanoparticles: An Up-to-Date overview. *Nanomaterials (Basel).* 2018;8(9):681. <https://doi.org/10.3390/nano8090681>
10. Xu L, Wang YY, Huang J, Chen CY, Wang ZX, Xie H. Silver nanoparticles: Synthesis, medical applications and biosafety. *Theranostics.* 2020;10(20):8996–9031. <https://doi.org/10.7150/thno.45413>
11. Swidan NS, Hashem YA, Elkhatib WF, Yassien MA. Antibiofilm activity of green synthesized silver nanoparticles against biofilm associated enterococcal urinary pathogens. *Sci Rep.* 2022;12(1):3869. <https://doi.org/10.1038/s41598-022-07831-y>
12. Bubonja-Šonje M, Knežević S, Abram M. Challenges to antimicrobial susceptibility testing of plant-derived polyphenolic compounds. *Arh Hig Rada Toksikol.* 2020;71(4):300–11. <https://doi.org/10.2478/aiht-2020-71-3396>
13. de Castro Melo P, Ferreira LM, Filho AN, Zafalon LF, Vicente HIG, de Souza V. Comparison of methods for the detection of biofilm formation by *Staphylococcus aureus* isolated from bovine sub-clinical mastitis. *Braz J Microbiol.* 2013;44(1):119–24. <https://doi.org/10.1590/S1517-83822013005000031>
14. Brown HL, Van Vliet AHM, Betts RP, Reuter M. Tetrazolium reduction allows assessment of biofilm formation by *Campylobacter jejuni* in a food matrix model. *J Appl Microbiol.* 2013;115(5):1212–21. <https://doi.org/10.1111/jam.12316>
15. Samreen, Qais FA, Ahmad I. Anti-quorum sensing and biofilm inhibitory effect of some medicinal plants against gram-negative bacterial pathogens: *in vitro* and *in silico* investigations. *Heliyon.* 2022;8(10):e11113. <https://doi.org/10.1016/j.heliyon.2022.e11113>
16. Kuete V, BertrandTepoño R, Mbaveng AT, Tapondjou LA, Meyer JJM, Barboni L, et al. Antibacterial activities of the extracts, fractions and compounds from *Dioscorea bulbifera*. *BMC Complement Altern Med.* 2012;12:228. <https://doi.org/10.1186/1472-6882-12-228>
17. Basson A, Flemming LA, Chenia HY. Evaluation of adherence, hydrophobicity, aggregation and biofilm development of *Flavobacterium johnsoniae*-like isolates. *Microb Ecol.* 2008;55(1):1–14. <https://doi.org/10.1007/s00248-007-9245-y>
18. Rosenberg M. Bacterial adherence to hydrocarbons: a useful technique for studying cell surface hydrophobicity. *FEMS Microbiol Lett.* 1984;22(3):289–95. [https://doi.org/10.1016/0378-1097\(84\)90026-0](https://doi.org/10.1016/0378-1097(84)90026-0)
19. Bose D, Chatterjee S. Biogenic synthesis of silver nanoparticles using guava (*Psidium guajava*) leaf extract and its antibacterial activity against *Pseudomonas aeruginosa*. *Appl Nanosci.* 2016;6(6):895–901. <https://doi.org/10.1007/s13204-015-0496-5>
20. Olojede SO, Lawal SK, Mahlangeni N, Shelembe B, Matshipi MN, Moodley R, et al. Synthesis and characterization of a conjugate of silver nanoparticles loaded with tenofovir disoproxil fumarate. *Next Nanotechnol.* 2024;5:100058. <https://doi.org/10.1016/j.nxnano.2024.100058>
21. Inamdar YM, Rane B, Jain A. Preparation and evaluation of beta sitosterol nanogel: A carrier design for targeted drug delivery system. *Asian J Pharm Res Dev.* 2018;6(3):81–87. <https://doi.org/10.22270/ajprd.v6i3.390>
22. Gerlier D, Thomasset N. Use of MTT colorimetric assay to measure cell activation. *J Immunol Methods.* 1986;94(1–2):57–63. [https://doi.org/10.1016/0022-1759\(86\)90215-2](https://doi.org/10.1016/0022-1759(86)90215-2)
23. Bolla SR, Mohammed Al-SA, Yousuf Al-JR, Papayya BJ, Kanchi RP, Veeraraghavan VP, et al. *In vitro* wound healing potency of methanolic leaf extract of *Aristolochia saccata* is possibly mediated by its stimulatory effect on collagen-1 expression. *Heliyon.* 2019;5(5):e01648. <https://doi.org/10.1016/j.heliyon.2019.e01648>
24. Yahaya A, Ali M, El-Hassan FI, Jido BL. Antibacterial activity of guava (*Psidium guajava* L.) extracts on *Staphylococcus aureus* isolated from patients with urinary tract infections attending a tertiary-care hospital. *Sci World J.* 2019;14(1).
25. Kenmeni JF, Sifi I, Bisso BN, Kayoka-Kabongo PN, Tsopmene UJ, Dzoyem JP. Exploring medicinal plants for antimicrobial activity and synergistic effects with doxycycline against bacterial species. *The Sci World J.* 2024;2024:6238852. <https://doi.org/10.1155/2024/6238852>
26. Lima JL da C, Alves LR, Paz JNP da, Rabelo MA, Maciel MAV, Moraes MMC de. Analysis of biofilm production by clinical isolates of *Pseudomonas aeruginosa* from patients with ventilator-associated pneumonia. *Rev Bras Ter Intensiva.* 2017;29(3):310. <https://doi.org/10.5935/0103-507X.20170039>
27. Mori S, Yamada A, Kawai K. Evaluation of the biofilm detection capacity of the Congo Red agar method for bovine mastitis-causing bacteria. *Jpn J Vet Res.* 2023;71(3):109–16.
28. Aishwarya SR, Beena AK, Aparna SV, Archana C, Aysha CH. Antibiofilm of *Enterococcus* sp. isolated from household thair sample. *J Vet Anim Sci.* 2024;55(1):57–64. <https://doi.org/10.51966/jvas.2024.55.1.57-64>
29. Borowicz M, Krzyżanowska DM, Jafra S. Crystal violet-based assay for the assessment of bacterial biofilm formation in medical tubing. *J Microbiol Methods.* 2023;204:106656. <https://doi.org/10.1016/j.mimet.2022.106656>
30. Venkatramanan M, Sankar GP, Senthil R, Akshay J, Veera RA, Langeswaran K, et al. Inhibition of quorum sensing and biofilm formation in *Chromobacterium violaceum* by fruit extracts of *Passiflora edulis*. *ACS Omega.* 2020;5(40):25605–16. <https://doi.org/10.1021/acsomega.0c02483>
31. Ghosh R, Tiwary BK, Kumar A, Chakraborty R. Guava leaf extract inhibits quorum-sensing and *Chromobacterium violaceum* induced lysis of human hepatoma cells: Whole transcriptome analysis reveals differential gene expression. *PLoS ONE.* 2014;9(9):e107703. <https://doi.org/10.1371/journal.pone.0107703>
32. Vasavi HS, Arun AB, Rekha PD. Inhibition of quorum sensing in *Chromobacterium violaceum* by *Syzygium cumini* L. and *Pimenta dioica* L. *Asian Pac J Trop Biomed.* 2013 ;3(12):954–59. [https://doi.org/10.1016/S2221-1691\(13\)60185-9](https://doi.org/10.1016/S2221-1691(13)60185-9)
33. Mogana R, Adhikari A, Tzar MN, Ramliza R, Wiart C. Antibacterial activities of the extracts, fractions and isolated compounds from *Canarium patentinervium* Miq. against bacterial clinical isolates. *BMC Complement Med Ther.* 2020;20(1):55. <https://doi.org/10.1186/s12906-020-2837-5>
34. Zhao A, Sun J, Liu Y. Understanding bacterial biofilms: From definition to treatment strategies. *Front Cell Infect Microbiol.*

- 2023;13. <https://www.frontiersin.org/journals/cellular-and-infection-microbiology/articles/10.3389/fcimb.2023.1137947/full>
35. Ashraf JM, Ansari MA, Khan HM, Alzohairy MA, Choi I. Green synthesis of silver nanoparticles and characterization of their inhibitory effects on AGEs formation using biophysical techniques. *Sci Rep.* 2016;6. <https://www.ncbi.nlm.nih.gov/pmc/articles/PMC4735866/>
  36. Asghar MA, Zahir E, Asghar MA, Iqbal J, Rehman AA. Facile, one-pot biosynthesis and characterization of iron, copper and silver nanoparticles using *Syzygium cumini* leaf extract: As an effective antimicrobial and aflatoxin B<sub>1</sub> adsorption agents. *PLoS ONE.* 2020;15(7):e0234964. <https://doi.org/10.1371/journal.pone.0234964>
  37. Ali IAM, Ahmed AB, Al-Ahmed HI. Green synthesis and characterization of silver nanoparticles for reducing the damage to sperm parameters in diabetic compared to metformin. *Sci Rep.* 2023;13(1):2256. <https://doi.org/10.1038/s41598-023-29412-3>